SCIENTIFIC CULTURE
www.sci-cult.com

SCIENTIFIC CULTURE, Vol. 6, No. 1, (2020), pp. 9-23
Open Access. Online & Print

DOI: 10.5281/zenodo.3483983

SPECTROSCOPIC CHARACTERIZATION OF PREPERATION, PIGMENT AND BINDING MEDIA OF ARCHAEOLOGICAL CARTONNAGE FROM LISHT, EGYPT

Hala A.M. Afifi[1], Rushdya Rabee Ali Hassan[2*], Mustafa A. Abd-EL-Fattah[3] and Shimaa M. Menofy[4]

[1,2,4]Restoration and Conservation Department, Faculty of Archaeology, Cairo University, 12613 Giza, Egypt
[3]General Director of Giza archaeological site, Ministry of Antiques, Egypt

Received: 09/09/2019
Accepted: 10/12/2019
Corresponding author: Rushdya Rabi Ali (rushdyarabii@yahoo.com)

ABSTRACT

The present study was applied on an archaeological cartonnage piece from lisht site to identify the chemical composition of the cartonnage materials and the damage forms that were resulted from buried soil. The examination process was implemented via the sampling techniques using Scanning electron microscope (SEM-EDS), X-ray diffraction (XRD) and Fourier transform infrared spectroscopy (FTIR). The results showed that the Egyptian blue (cuprorivaite), Egyptian green and red ocher were used as the pigment layer. The linen was used as a textile layer and calcium carbonate (calcite) as the preparation layer. The gum Arabic used as an organic media which was used in all layers as a binder of the cartonnage component. These materials suffered from the effect of surrounding environmental conditions in lisht especially the effect of diversity in the air temperature that was influenced the object tensile strength and caused a general weakness of all layers. It also caused shrinkage and wrinkle to the textile layer. Microbiological tests were performed for two swabs from the pigment layer and the textile layer to identify the bacteria and fungi species which affected the cartonnage material. Burkholderia Sp. was identified on the red pigment surfaces and the textile layer. Burkholderia Sp., bacteria species usually convert cellulose and hemicelluloses polysaccharides into a saccharified solution containing mixed sugars that used as a carbon source. This process plays a role in promoting The microbiological damage Which damages the organic material properties and caused the surface staining

KEYWORDS: Lisht site, Archaeological Cartonnage, X-ray diffraction, Scanning electron microscope (SEM)

1. INTRODUCTION

As a result of the ancient Egyptian beliefs in resurrection and immortality, many industries evolved to serve this concept. This belief led them to saved their dead bodies by mummify- cation, buried their dead in fortified tombs built in the desolate desert and provide the graves with all the food, drink and Tools to be used after the resurrection (Taylor, 2001).To confirm this belief, the ancient Egyptians assumed several elements that no one has to live without in the other life such as body, Heart, shadow, name, soul and soul mate (Asante, 2014), The ancient Egyptians were concerned with each unit separately, besides taking care of it as one unit, so, body and heart were preserved using embalming, soul recites hymns in order to protect it and the soul mate (ka) represented as hands raised above the head of the dead. They believed that the soul mate (ka) was associated with soul by order of the god (Ra) and as long as the (ka) joined him then he is alive. In order to the soul recognize her body, ancient Egyptian in old Kingdom made statue of plaster and put it at the beginning of the graveyard, This method developed in the five Dynasty of Egypt to take the known form of Cartonnage, which began with simple plaster masks and continued to develop to be free of defects until it reached the full mask of the body (Wallis, 1899). The Cartonnage masks consists of Composite layers arranged from top to bottom with pigment layer, sometimes was gilded followed by preparation layer called gesso which consist of calcium carbonate (calcite) or gypsum, finally textile layer consists of linen, papyrus or straw and clay. The artist occasionally used two of them together as linen and papyrus, straw and clay (Scott, 2003). Artists using binding media to tie layers together such as gum Arabic (AL- Emam et al., 2015) and Animal glue (Ali, 2016; Afifi, 2011; Scott et al., 2008).

The main periods in which the Cartonnage was used in Egypt were the Middle Kingdom (2025 –1700 BC), New kingdom period (1550 – 1070 BC), Third Intermediate Period (1069 – 664BC), Ptolemaic and Early Roman Periods (Fig.1.B) (Nassef et al., 2016).

In the Middle Kingdom, Cartonnage was made similar to the size of the real face then it evolved to the neck area. The masks were painted in blue and yellow and then are gilded (Hassaan, 2016). Cartonnage continued to be used in the New kingdom period and flourished again. It characterized by bright colours and decoration and the shape extended to the chest area and arms. By the end of the period, the Cartonnage had covered the entire body either flat or three-dimensional (Fig. 2. A) (Dodson, 2011).

In Third Intermediate Period, Cartonnage was made by making an inner layer of clay and straw, which is constructed by laying layers of plaster and linen similar papier-mâché technique. Anew type was also discovered at the end of this period and still used in the beginning of the Roman period, this type was made of colored glass beads (Fig.3.D) (Corcoran, 2014).

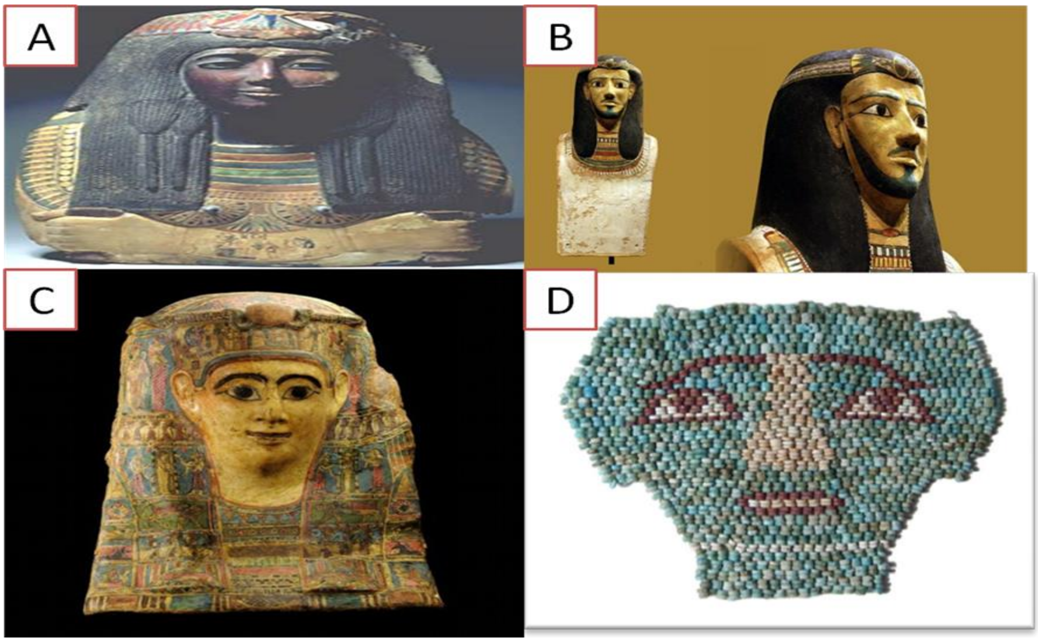

Figure 4. (A, B, C, D) (A) archaeological Cartonnage mask for a woman return to 19 dynasty, (B) archaeological Cartonnage piece dating back to The Middle Kingdom, Walters Museum in Pal Timor, according to (Hassaan, 2016), (C) mask dating back to the Greco-Roman era published at Christie's in New York, according to (Rifai, J, 2013, (D) Cartonnage piece made of colored beads.

The Roman era witnessed the flourishing of Cartonnage, it received great interest and became a mixture of Hellenistic art and Egyptian art which came as a result of the faith of the Greeks and Romans in the Egyptian beliefs (Fig.5.C) (Scott, 1998). The Cartoonage industry deteriorated in the Ptolemaic period and became less common from the 25th Dynasty until it disappeared in the 7th century BC and was replaced by wooden interiors. In this period, a new simpler method of mummy decoration was adopted. Instead of encasing the mummy in a one-piece mummiform shell, there was a cartonnage of six pieces, which sometimes increased to eight pieces. The pieces were decorated with colored sheets, which were fixed in their places by clasps or ribbons (Afifi, 2011). These masks buried with the mummy in a graveyard or directly in the soil like the sample object which was found in Lisht site, and as a result of buried it directly in the soil, the material affected by the site conditions which necessitated us study climatic conditions in it.

1.1 Lisht archaeological site

Lisht is a famous archaeological site located 65 kilometres south of Cairo on the left bank of the Nile (Fig. 6). It was raised to prominence position during the Middle Kingdom (12th Dynasty) (Willoughby, 2012) since Amnemhat I came to power and named it Itj-Tawi which means the one that seizes the two lands (Wegner, 2010). The first formal excavation in the site began in 1882 by French Mission. From 1906 to 1934, the Egyptian Expedition of the Metropolitan Museum, New York continued to work in the site (Arnold, 2008). Through excavating, archaeologists able to learn a few things from the excavation object, even if the remains were not in Perfect case like the object case. The investigated samples are part of Cartonnage piece was discovered in Lisht site and preserved in archaeological store without any restoration process. It described as Cartonnage piece from the chest area decorated with geometric motifs and painted with blue, green and red pigments (Fig. 7.A, B). It consisted of composite layers arranged from top to bottom, with the pigment layer, the preparation layer (gesso) and the support layer.

The visual examination showed some deterioration manifestations occurred as a result of burial in lisht soil which included physical, chemical and biological changes such as shrink, wrinkle of the textile layer, cracks and micro-fractures of the pigment and the ground layer, crumbling of some parts of the pigment and the ground layer and stains on red pigment layer and textile layer (Fig. **1**.B). These forms of damage caused by several conditions such as the effect of air temperature and humidity.

From the air temperature average per month for Lisht site we can notice that there is diversity in the air temperature degrees. In the winter, the temperature reaches 13C in January and rise slowly in February and March till June and reach 27.3C (Fig. 8). It also returns to decrease again the remaining months of the year (Fig. 9). The air temperature is associated with prevailing humidity in the archaeological site which comes from many sources like rainfall, Water which was used for irrigation of agricultural lands adjacent to archaeological sites. The relative humidity in lisht reach 83% in winter and decrease to 65% in summer according to freemeteo. co.il, (2018).

By connecting the previous factors with each other We can see that if humidity average decrease and the temperature average rise, the moisture content will evaporate and cause dehydration to the textile, Also it Contributes to break the Chemical bonds of the binding media.

In the winter, the decrease of temperature and the increase of relative humidity has the power to dissolve the binding organic media which was used in the pigment layer and leads to a displacement the layer. It also encourages microbiological growth that produce some organic acids which have the power to dissolve the components of the material and make stains on the archaeological material surfaces. These factors also contribute to making big variation when salts found in soil. when the air temperature levels rise, the salt will crystallize and when the air temperature decrease salts will be dissolved and reconstituted in other places causing damage to the archaeological material In several forms such as cracks.

From this point, the study analyzed some fragments from the painted Cartonnage and identified the damage factors which resulted from the burial environment in Lisht as prelude to initiate experimental study and choose the suitable conservation materials when dealing with.

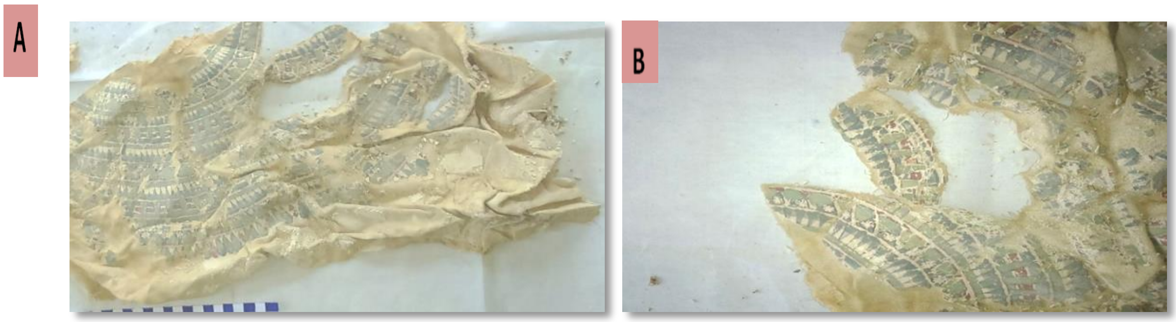

Figure 10. (A,B) Studied excavated Cartonnage.

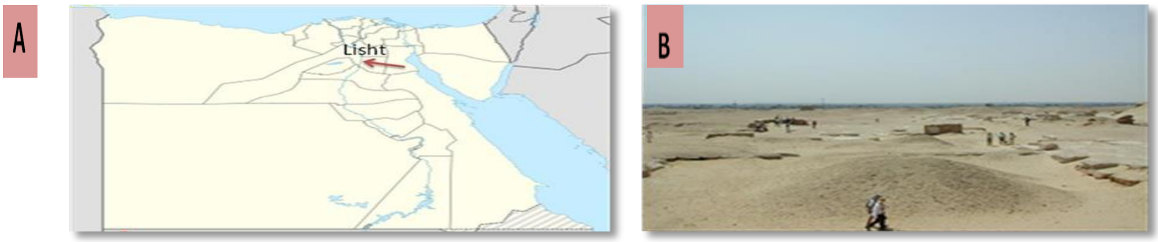

Figure 11. The area of excavation work and the location of Lisht on the map.

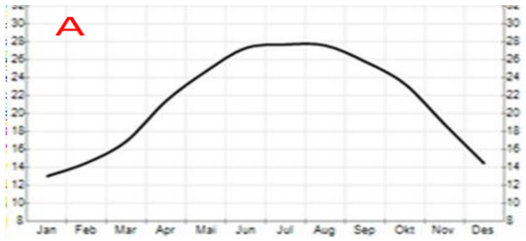

B	Temperature		
Months	Normal	Warmest	Coldest
January	13.0°C	-	-
February	14.5°C	-	-
March	16.9°C	-	-
April	21.4°C	-	-
May	24.7°C	-	-
June	27.3°C	-	-

Figure 12. (A, B) the air temperature average per month, Lisht sit.

2. MATERIALS AND METHODS

Samples from falling parts were examined and analyzed to indicate nature and damage to the Cartonnage material. For this purpose, some methods of examination and analysis were used such X-ray diffraction, Digital microscope, Scanning electron microscope and Fourier transforms infrared spectroscopy.

- ***Digital microscope (Dino -lite)***
  Dino Capture 2.0 with Version 1.5.12 was used to study the sample surfaces such as colour, and texture of the layer, as well as the surface's degradation such as Stains and cracks.
- ***Scanning electron microscope (SEM-EDX)***
  Chemical composition of archaeological cartonnage materials were determined using scanning electron microscope (SEM) (Quanta 200 manufactured by FIE), equipped with energy dispersive X-ray spectrometer (EDX) unit with detector model 6587, Mag: 2400, resolution at 124.4 eV, Accelerating voltage 25 KV.
- ***X-ray diffraction (XRD***
  The samples were analyzed by Philips PW3209 Diffractmeter, Manufactured by PA. Analytical. The pattern was running continuously using Anode material Copper (Cu) in General setting 30 mA & 40 KV.
- ***Fourier transforms infrared spectroscopy (FTIR)***
  The Samples were analyzed as KBr pellets using the Bruker-model vertex 70, with a spectrum ranging from 400 cm^{-1} to 4000 cm^{-1}, at resolution 4 cm^{-1}. This method was used to identify functional groups of the binder.
- ***Matrix-assisted laser desorption ionization time-of-flight mass spectrometer (MALDI-TOF)***
  Blood agar media and MacConkey (MAC) agar were used in the isolation and cultivation of micro-organisms isolated from pigment layer and textile to identify them using (MALDI-TOF) mass spectrometer.

3. RESULTS AND DISCUSSION

3.1 *The textile layer*

Topography of the textile layer was studied using digital microscope. The result revealed that the fabric layer is one textile layer (Fig.13.A), the examination showed the discoloration of some places; especially the external parties which turned to brown colour and burned in some places (Fig.14.C). The main reason for the discoloration of archaeological textiles could be as result of darkness of gum Arabic according to (Abd-Elghani, 2009). Also, (Cybulska, 2007) says the textile become degraded during prolonged burial and are already fragile and weakened when excavated. Another reason was describe by (Ali et al., 2017), she mentioned that colour change from dark brown to black may be due to thermal degradation of the textile fibers. All pervious reasons could be Gathered with biological degradation and played role in degradation process. The effect of these organisms appeared in the form of organic color spots on the red layer and the textile layer. The effect of the soil was also showed when the piece was examined, dryness and fragmentation of the colours and preparation layer and the textile layer was appeared.

When the textile layer was examined using SEM, the fibres appeared under a microscope as soft cylindrical strap characterized by occasional incisions at the place of swelling, which referred to the linen textile (Fig.15.A). When the fibres were examined, some strange crystals were observed. Then analyzed elements of (Al), (Mg), (O), (Si), (MO), (Ca), (Fe), (CL) emerged, which belong to sand soil (Fig. 16).

FTIR spectrum of the textile layer compared to references of Arabic gum and linen textile. According to((Derrick et al., 1999).band of Arabic gum were shown at 3280 cm^{-1}, 3381 cm^{-1}, 2918 cm^{-1}, 1620 cm^{-1} , 1420, along with methyl and ethyl bonds which characterize cellulose appeared at 1374 cm^{-1}, 1338cm^{-1}, 1028 cm^{-1} and 1248 cm^{-1}, C-O stretching band appeared at 1028 cm^{-1} and 1248 cm^{-1} in the textile layer only which referred to lignin. In the last O-H bending band was appeared in textile layer only at 1620cm^{-1} (Fig.17).

Figure 18. (A, B, C) (A, B) digital microscope of textile layer. (C) SEM micro photos of the textile layer.

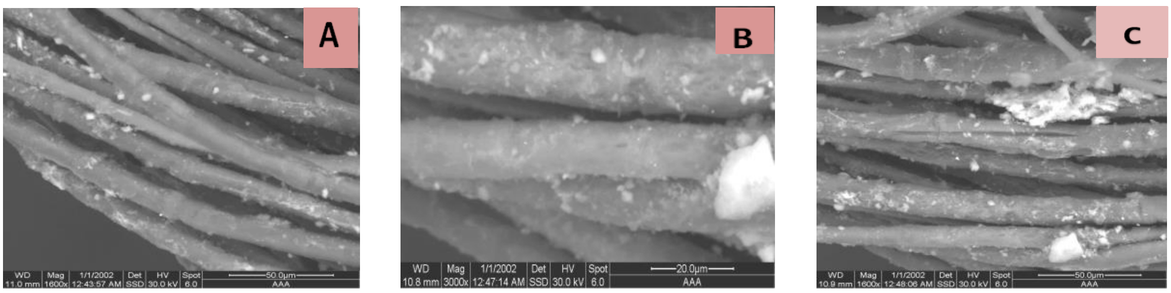

Figure 19. (A, B,C) SEM micro-photos of the textile layer.

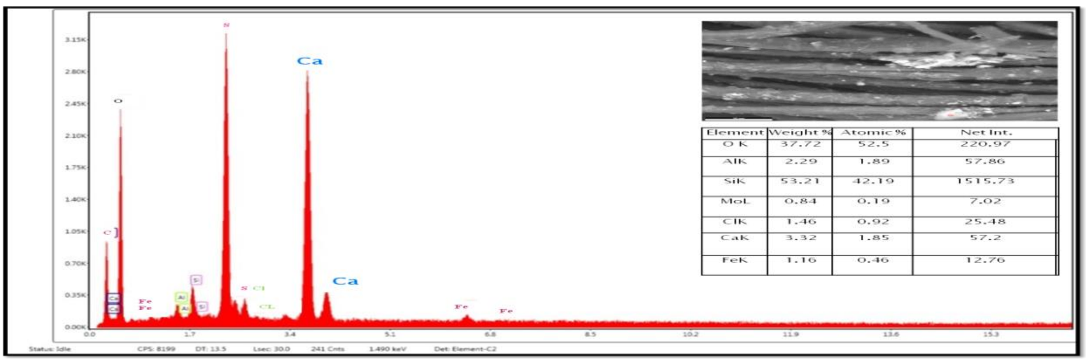

Element	Weight %	Atomic %	Net Int.
O K	37.72	52.5	220.97
AlK	2.29	1.89	57.86
SiK	53.21	42.19	1515.73
MoL	0.84	0.19	7.02
ClK	1.46	0.92	25.48
CaK	3.32	1.85	57.2
FeK	1.16	0.46	12.76

Figure 20. EDX data of the surface of the fibres.

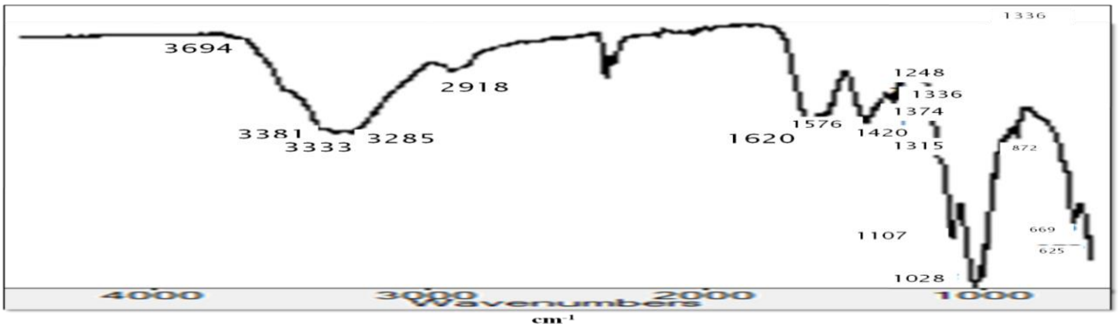

Figure 21. FTIR patterns of the textile layer.

3.2 *The preparation layer*

Plaster layer was employed in the Cartonnage as preparation layer on the pigment layer. The layer made of calcite ($CaCO_3$) mixed with Arabic gum with traces of magnesium, silica and alumina revealed by Optical microscope, SEM-EDX, XRD and FTIR analysis (Fig.22, 23, 24, 25). To provide a clear picture of the investigated sample compounds, XRD was applied on powdered fragments to give information about the structure of crystalline materials. The available resulting spectra were presented in (Fig.26) Where the peaks were assigned and identified using PA analytical XRD analysis software with atypical reference database. Qualitative identification indicated the existence of calcite.

The characteristic shape of the calcite granules showed up using SEM microscope it takes the cubic shape (Fig.27.C) mentioned by (Ni and Ratner, 2008).

FTIR allowed to recognition of the characteristic band of Arabic gum which used in the layer mixed with calcite. The bands of Arabic gum were identified at 3433 cm^{-1}, 2921 cm^{-1}, 2870 cm^{-1}, along with the bands of calcium carbonate (calcite) at 1422cm^{-1}, 874cm^{-1}. Some peaks of Arabic gum were shifted to the right and O-H bending band; C-H bending band and C-O stretching band were disappeared from chart (Fig. 28) (Table.1). This change could be due to the overlap of some picks of calcium carbonate on the Arabic gum peaks, the other possibility was the effect of surrounding damage factors especially the effect of the high temperatures which shifted the functional groups until it Completely disappeared, this action leads to breakdown the mechanical properties which caused loss of binding media function (Daoubab et al., 2018).

These results illustrated the similarity of the Chemical composition and the Physical properties such as Color and granular shape of the sample which belong to calcite and the presence of aluminum (Al) and silica (Si) could be from dust particles and the presence of (Mg) Owed to lime stone which had been used in makes lime (Fig.29) (Abd El-Tawab et al., 2012).

Calcite considered one of the important material used in the Cartonnage preparing layers to give soft and flat layers to apply the paint directly. It found on many Cartonnage pieces but mostly mixed with another compounds not as the study case, which appeared in the form of a single layer of calcite.

According to Afifi, (2011) and Hussein et al. (2019) calcite appeared as a basic component of the preparation layer which consist of two layer, coarse layer covered with another smooth layer prepared for painting process, the inner coarse ground layer is composed of calcite $CaCO_3$ as a major with small amounts of quartz (SiO_2) and the fine ground layer used under the pigments directly was composed of calcite, CaCO3 only. It also was identified by (Abd El-Tawab et al., 2012) who examined the plaster layer and the results indicated that they were mainly consists of calcite (CaCO3) based plaster, with peaks matching Gypsum ($CaSO_4$) and quartz (SiO_2) together with some suggestion of the presence of Kaolinite ($Al_4(Si_4O_{10})$ (OH) and when Abd El et al., (2014) examined the preparation layer of archaeological Cartonnage found in Saqqara, the results showed that it consists of two layers The first Coarse ground layer being mixture of calcite and huntite and The second layer (finer one) being pure white calcite.

The above mentioned results, show the prevalence of the use of calcium carbonate throughout the ancient Egyptian as a mixture or alone as the study subject Cartonnage.

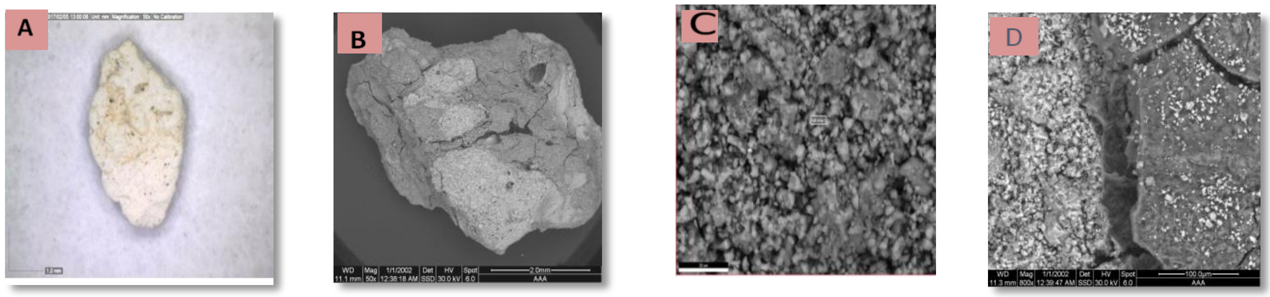

Figure 30 (A,B,C): (A) digital microscope of the prepration layer of the cartonnage fragment. (b) SEM micro photos of the sample. c) SEM micro photos of calcite cubic shape, (D) SEM micro photos of the physical damage

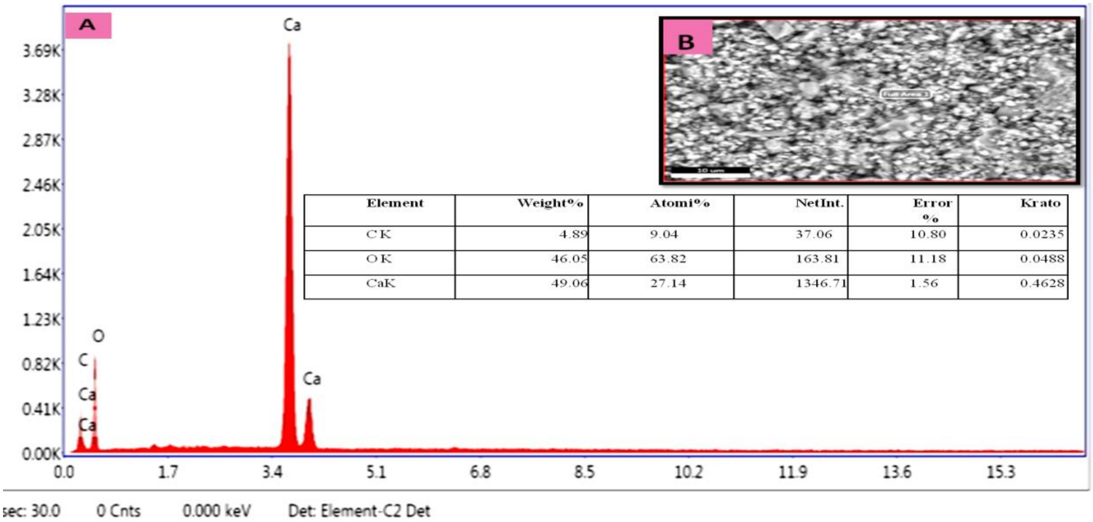

Element	Weight%	Atomi%	NetInt.	Error %	Krato
C K	4.89	9.04	37.06	10.80	0.0235
O K	46.05	63.82	163.81	11.18	0.0488
CaK	49.06	27.14	1346.71	1.56	0.4628

Figure 31. SEM-EDX pattern of the prepration layer.

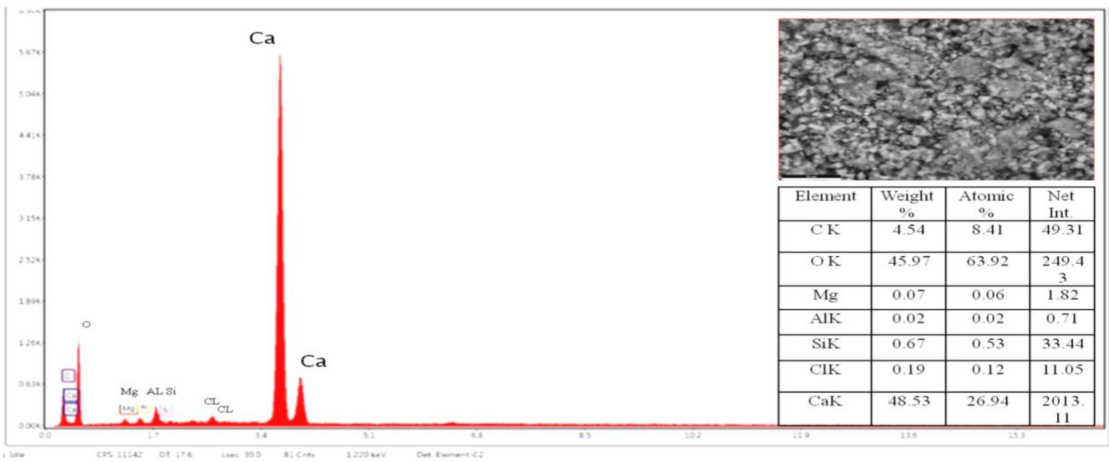

Element	Weight %	Atomic %	Net Int.
C K	4.54	8.41	49.31
O K	45.97	63.92	249.43
Mg	0.07	0.06	1.82
AlK	0.02	0.02	0.71
SiK	0.67	0.53	33.44
ClK	0.19	0.12	11.05
CaK	48.53	26.94	2013.11

Figure 32. (A,B) SEM- EDX pattern through the cracks that appeared in the preparation layers.

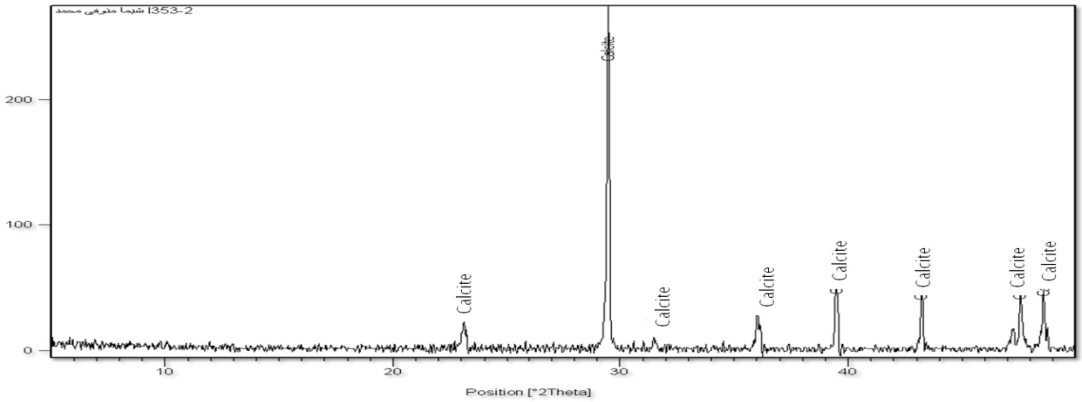

Figure 33. XRD pattern of the preparation layer.

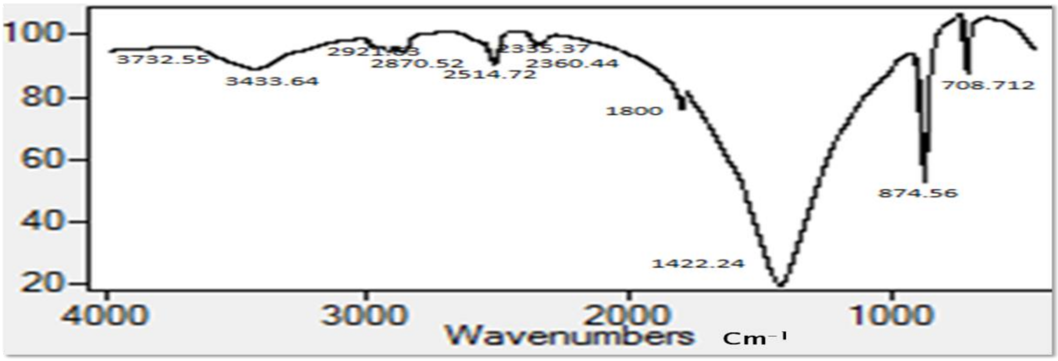

Figure 34. FTIR pattern of the preparation layer.

Table 2. Infrared Absorption of the preparation layer

Functional group of Arabic gum	Sample wave number
O-H Stretching band 3600-3200cm^{-1}	----- 3433
C-H Stretching band 3000-2800 cm^{-1}	2921
O-H bending band 1650-1850 cm^{-1}	1800
C-H bending band 1480-1300 cm^{-1}	-------
C- O Stretching band 1300-900 cm^{-1}	-------

3.3 The pigment layer

The pigments can be defined as a component of a paint that contributes colour. This is usually dry and solid. To produce a paint, the pigment must be mixed with a binder which is typically an organic compound such as gum Arabic, various plant-derived oils, wax, egg-yolk and many others else (Siddall, 2018).

To identify the pigments which were used in the Cartonnage, the pigments were analyzed using SEM providing with Energy Dispersive X-Ray Spectroscopy. From the naked eyes examination to pigment layer we can notice that it consists of three pigments, Blue, green and red.

Blue pigment particles with different shades from dark blue to Blackish blue were revealed using the optical microscope (Fig.35.A). SEM micrograph showed characteristic particles of cuprorivaite (Hussein et al., 2019) in the first and second and sample (blackish dark) and the cubic calcite crystals also showed (Fig.36.C).

The EDX examination of both samples showed that the blue pigment consisted of Carbon (C), oxygen (O), silica (Si), (S), (Ca), (Fe), (Cu), (K), (CL), (Na)(Fig. 37, 38) this elements revealed composition comprises Egyptian blue ($CaCuSi_4O_{10}$). The visual examination, dino-lite photography, and SEM micrographs of the E.B pigment proved that the pigment appearance turned to dark in some parts (Fig. 39). In this context, (Abdel-Ghani, 2009) explained some of the reasons for this change which included dust effect deposited on the paint surface or trapped within a thin layer of a calcium sulfate crust formed by the reaction between atmospheric vapor and calcium carbonate substrate of the painting. In addition, (Daniels et al., 2004) noted that the main cause of this phenomenon is the darkening of media by the time.

The Egyptian blue or cuprorivaite described as a synthetic pigment appeared during the third millennium BC. It used throughout the Dynastic period particularly in the Roman era (Gimenez, 2015; Coccato, 2017; Al-Emam et al., 2015; Moussa and Ali, 2013; Katsaros et al., 2010; Siddall, 2006; Camagna et al, 2003; Mazzocchin et al., 2003; Weatherhead and Buckley, 1998). It was made by mixing lime or limestone with silica source (sand) and copper compounds (Copper oxides and cuprite or tenorite) with flux (Panagopoulou et al., 2016; Mahmud, 2010; Pages-Camagna and Colinart, 2003) and was manufactured at temperatures from $800^{o}C$ to $1050^{o}C$ (Moussa, 2013; Accorsi et al., 2009; Berke, 2007). His prosperities were stable to acids, alkaline and light (Berke, 2007).

The second pigment is green paint which recognized during visual examination. The optical microscope image showed pale green shade with low coverage (Fig.40). When it was analyzed with EDX (C), (O), (Si), (S), (Ca), (Na), (Cu), (Al), (Cl), (K) was appeared which referred to the Egyptian green pigment (Fig. 41).

The EG is synthetic pigment viewed as a pale EB produced at $1500C^{o}$ that makes his properties diverse Compared with EB although the fact they have a similar compound (Die-Stefano and Fuchs, 2011; Hatton et al., 2008; Pagès-Camagna et al., 1999; Pagès-Camagna and Colinart, 2003; Tite, 1987).

The red paint appeared under optical microscope tends to light (Fig. 42, A), when it analyzed, the results of the red pigment elucidated that pigment consists of (C), (O), (Si), (S), (Al), (S), (Ca), (Cl), (K), (Fe) elements (Fig.43) Which is known as red ocher according to (Mahmuod & Papadopoulos, 2013; Mahmoud, 2010; Gutman et al., 2010; Iriarte et al., 2008).

Ocher usually used as a generic term of any rock, earth or mineral producing a reddish or yellowish streak when abraded and containing iron oxide (Montalto, 2010; Watts, 2009) like yellow ocher which heated at temperatures ranging from 300°C to 900°C (Uda et al., 2000). It also produced from goethite (αFeO.OH), hematite (α-Fe2O3), white pigments (alumina-silicate as Kaolinite, Illite, quartz) and calcium compounds (calcite, gypsum, anhydrite) (Abdel-Ghani, 2009). It can be distinguished by many features, red ochre is characterized by the presence of silica and alumina and given a light red color when examined under digital microscope. SEM investigation for three different places in the preparation layer which appeared in the red paint sample showed some holes and organic stains (Fig.44, 45) (Fig.46.A, B). The organic stains confirmed the effect of biological damage and his role in damage process by produced enzymes that resulted Colour spots on the pigment surface and destroyed the organic layer component. FTIR analysis was performed on powdered sample of the all pigment layer paints, from analysis result we can recognize functional group of Arabic gum which mixed with the pigments as binder. The functional groups peaks were recognized at $3425cm^{-1}$, $2974cm^{-1}$, 2923 cm^{-1}, 2870 cm^{-1}, $1800cm^{-1}$ with the functional group of calcium carbonate which used in preparation layer and his peaks appeared at 1422 cm^{-1}, 873 cm^{-1} . we couldn't recognized any pigment which mixed with preparation layer. when we grinded the sample the thickness of the pigment layer was very thin Which could not be examined alone (Fig. 47)

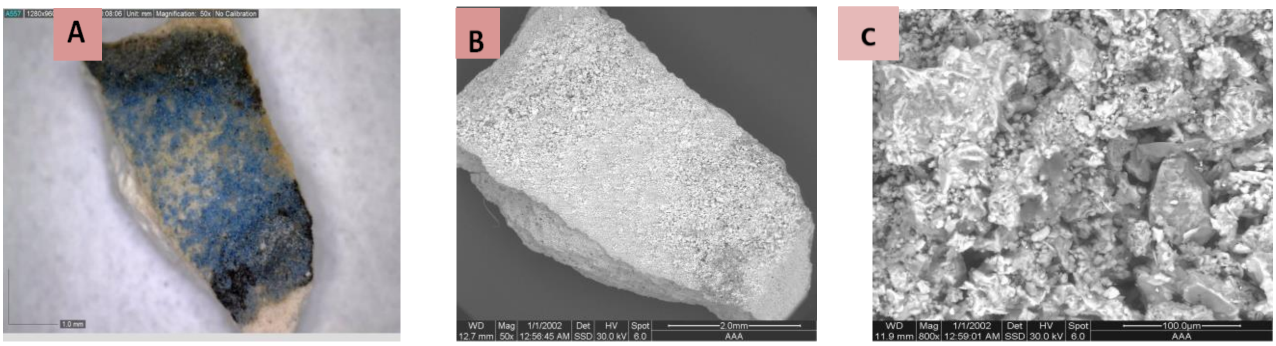

Figure 48. (A,B,C)(A) digital microscope photo of blue pigment layer, (B, C)SEM micro photos of the blue pigment surface and grains.

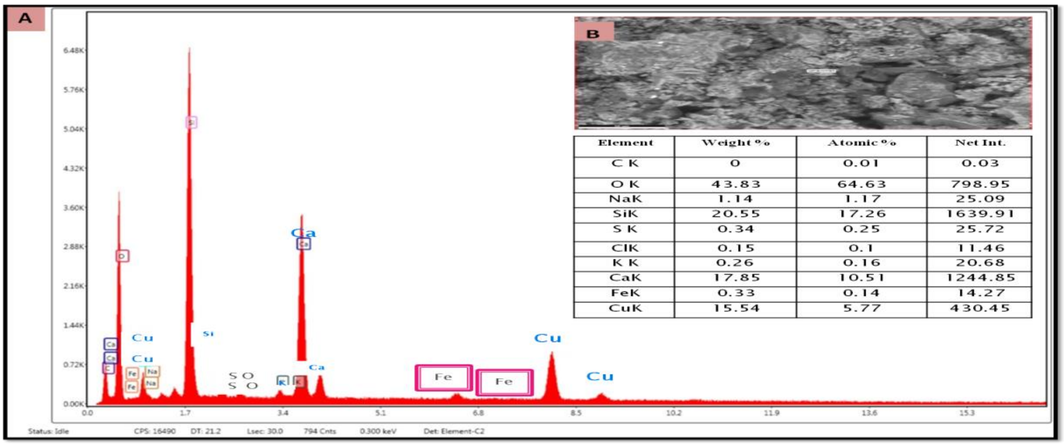

Figure 49. (A, B) SEM-EDX patterns of blue pigment.

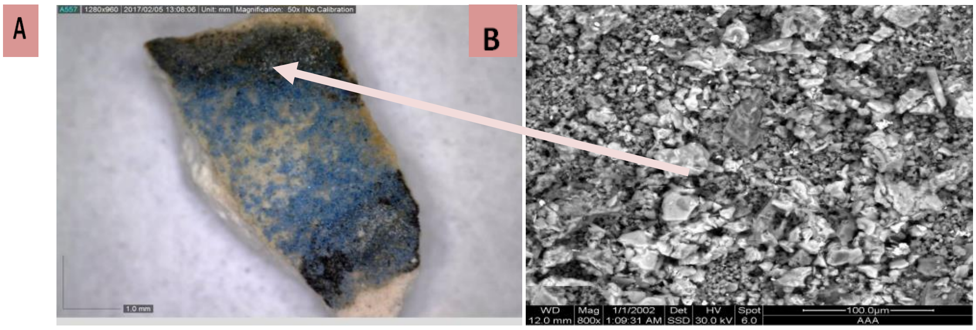

Figure 50 (A,B): (A) digital microscope photo of blackish blue pigment layer, (B) SEM micro photos of the blue pigment surface and grains.

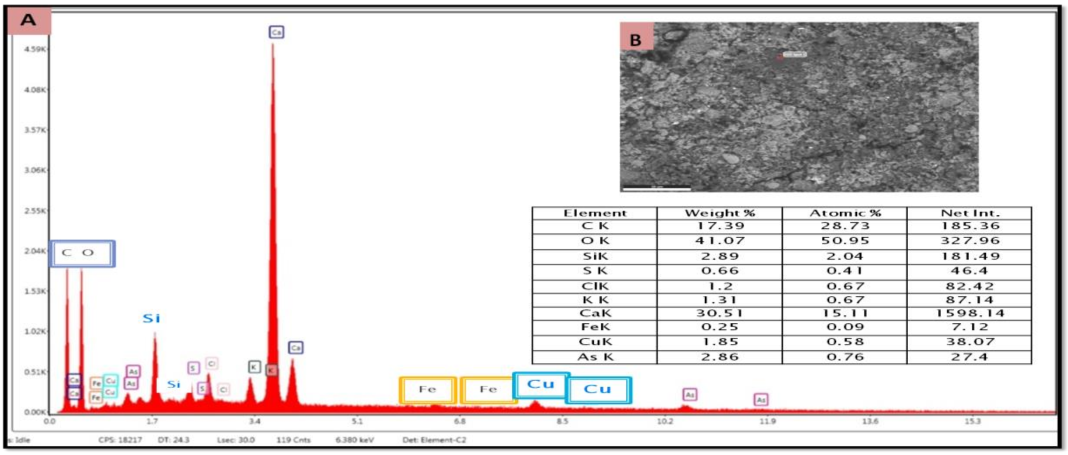

Figure 51 (A, B): SEM-EDX patterns of the blackish blue pigment.

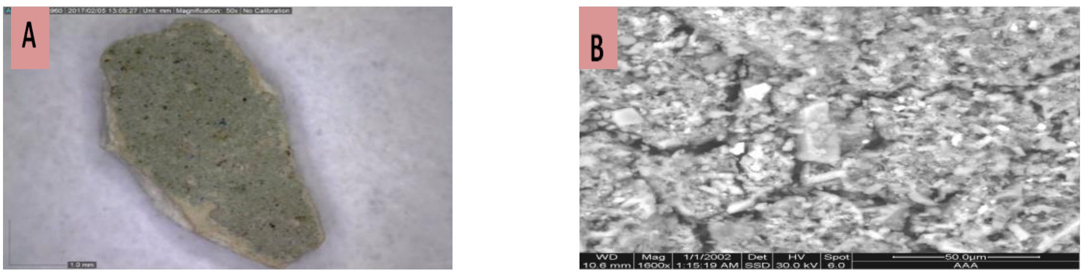

Figure 52 (A,B): (A) Digital microscope photo of green pigment layer, (B) SEM micro photos of green pigment grains.

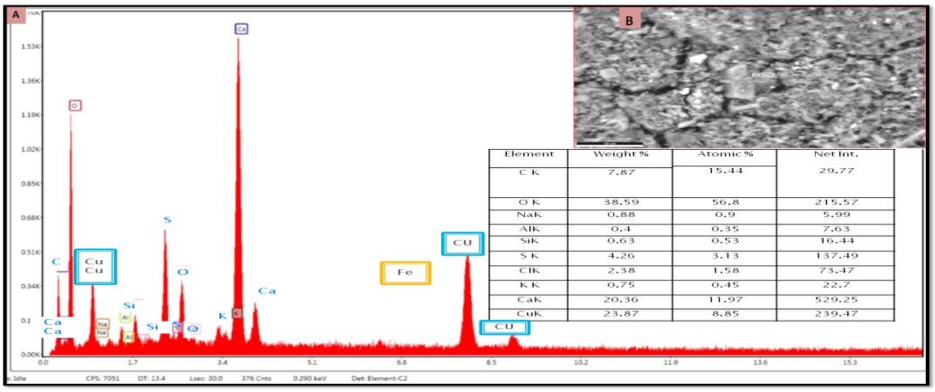

Element	Weight %	Atomic %	Net Int.
C K	7.87	15.44	29.77
O K	38.59	56.8	215.57
NaK	0.88	0.9	5.99
AlK	0.4	0.35	7.63
SiK	0.63	0.53	16.44
S K	4.26	3.13	137.49
ClK	2.38	1.58	73.47
K K	0.75	0.45	22.7
CaK	20.36	11.97	529.25
CuK	23.87	8.85	239.47

Figure 53: (A, B) SEM-EDX patterns of the green pigment.

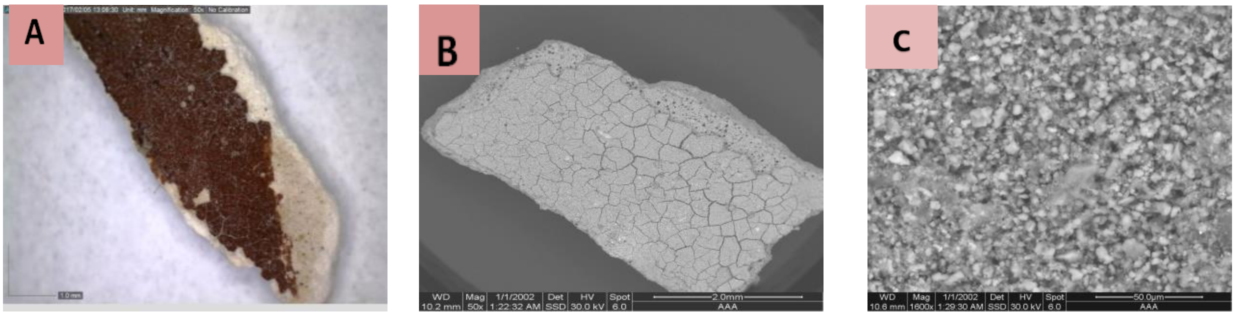

Figure 54 (A,B,C): (A) digital microscope photo of blue pigment layer, (B, C)SEM micro photos of the blue pigment surface and grains.

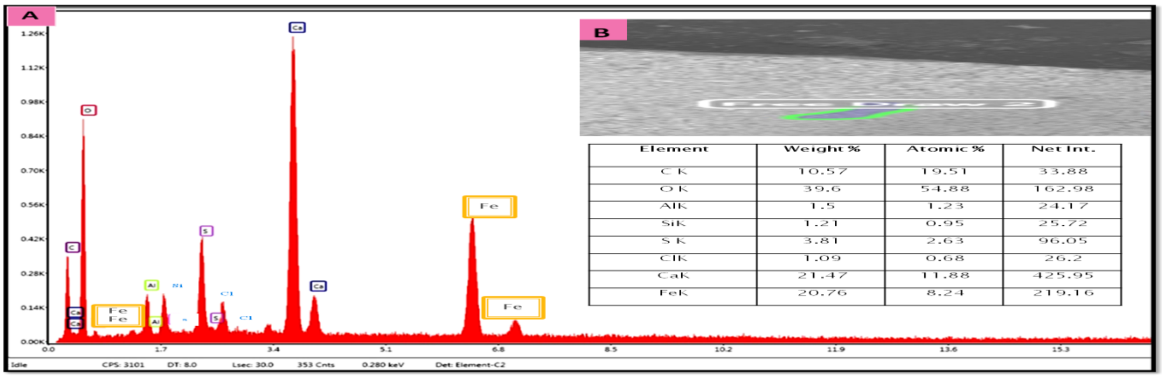

Element	Weight %	Atomic %	Net Int.
C K	10.57	19.51	33.88
O K	39.6	54.88	162.98
AlK	1.5	1.23	24.17
SiK	1.21	0.95	25.72
S K	3.81	2.63	96.05
ClK	1.09	0.68	26.2
CaK	21.47	11.88	425.95
FeK	20.76	8.24	219.16

Figure 55 (A, B): SEM-EDX patterns of the green pigment.

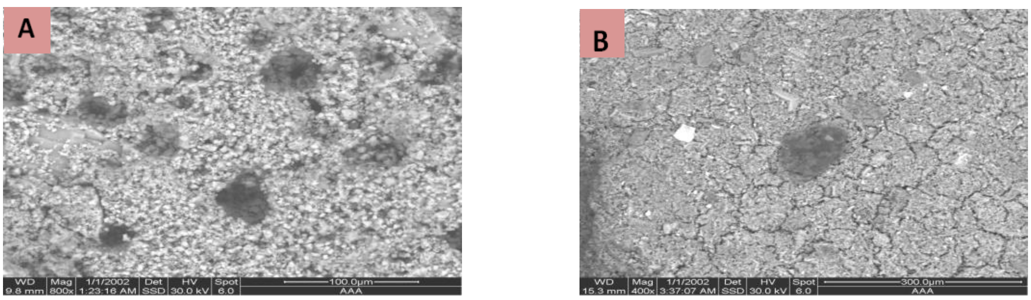

Figure 56 (A, B): SEM micro-photos of the holes and stain on red pigment.

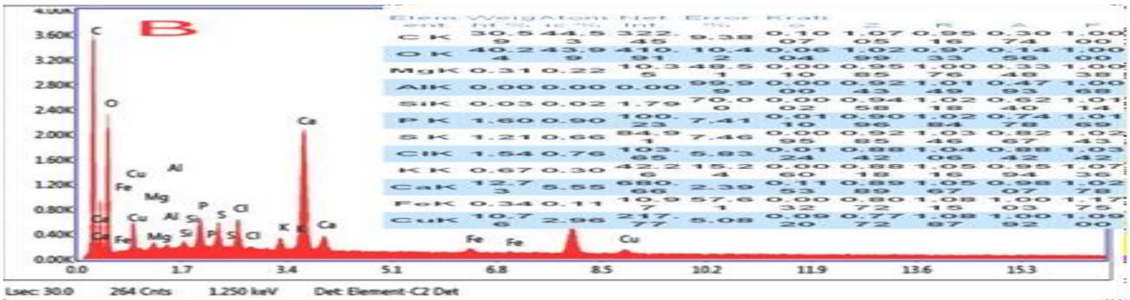

Figure 57. EDX of organic stains on red pigment samples. (A) SEM micro photos of the stains on red pigment layer. (B) EDX data of the organic stains

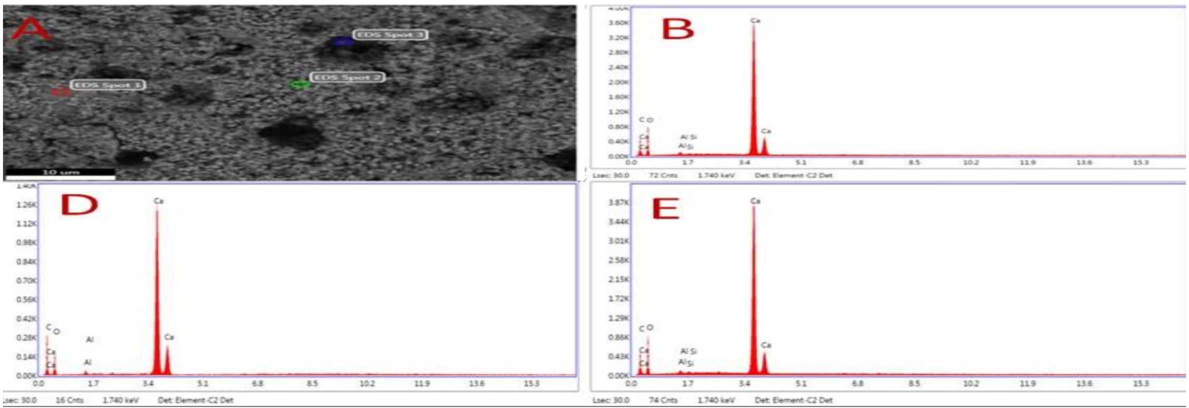

Figure 58. (A) SEM micro photos the holes. (B, D, E)EDX of the holes appeared in the red pigment layer.

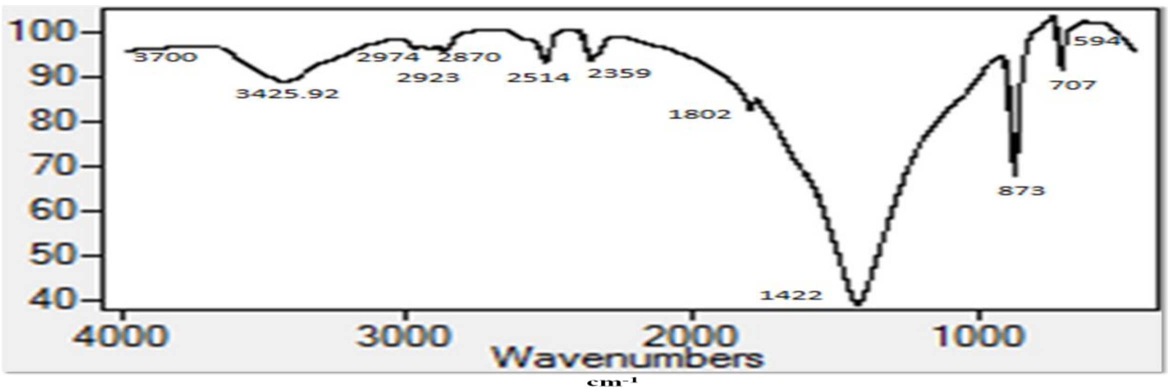

Figure 59. FTIR patterns of the pigment layer.

4. CONCLUSION

The results obtained by the qualitative and quantitative techniques (EDX, FTIR and XRD) concluded that the cartonnage piece consisted of three layers, the first layer is pigment layer which was consisted of the Egyptian blue, the Egyptian green and red ocher. The second layer was composed of calcite, which was placed on a linen layer that came as the last layer. The study's results also refers to the effect of the damage factors in Lisht site, especially variety of the temperature degree which is considered the most aggressive degradation factor on dry soil. This effect appeared in several forms like weaknesses, cracks that observed in pigment and ground layer, discoloration of some pigment appearing like the darkness of Egyptian blue in some parts, shrinkage and wrinkle of the linen layer. Also, it has an impact on increasing the biological damage which caused the surface staining and decomposition the organic material.

REFERENCES

Abd El-Tawab, N., Bader, N., Mahran, A., (2012) Analytical investigation of Cartonnage fragment from late period. *Egyptian Journal of Archaeological and Restoration Studies* "IJARS", Volume 2, Issue 2, pp. 69 78.

Abdel-Ghani, M.H. (2009) A Multi-instrument Investigation of Pigments, Binders and Varnishes from Egyptian Paintings (AD 1300-1900): Molecular and Elemental Analysis Using Raman, GC-MS and SEM-EDX Techniques, PhD, Department of Archaeological Sciences, University of Bradford, West Yorkshire, England. http://hdl.handle.net/10454/4315.

Abu-Baker, A., Al Sekhaneh, W., Shiyab, A., Dellith, J., Scheffel, A., Alebrahim, M.A. and Popp, J. (2014) Analytical investigation of five roman pb-based scale weights (Qasr Ar-Rabbah, Jordan): A case study, *Mediterranean Archaeology and Archaeometry*, Vol. 14, No. 1, pp. 181-190.

Accorsi, G., Verri, G., Bolognesi, M., Armaroli, N., Clementi, C., Milani, C. and Romani, A. (2009) The exceptional near- infrared luminescence properties of cuprorivaite (Egyptian blue). *Chem. Common*, (23), pp. 3392-3394.

Afifi H.A.M (2011) Analytical Investigation of Pigments, Ground Layer and Media of Cartonnage Fragments from Greek Roman Period. *Mediterranean Archaeology and Archaeometry,* Vol. 11, No. 2, pp. 91-98.

Akita, H., Kimura, Z., Zulkhairi, M., Yusoff, M., Nakashima, N., and HoshinoIsolation, T. (2016) characterization of Burkholderia sp. strain CCA53 exhibiting ligninolytic potential, Springer plus, 5: 596 https://www.ncbi.nlm.nih.gov/pmc/articles/PMC4864794/

Ali, M.F., Mansour, M.M.A., Badr, N.M. and Salem, M.Z.M (2017) A Study of Biodeterioration and Chromatic Alterations of Painted and Gilded Mummy Cartonnage at the Saqqara Museum Storeroom, Egypt, *Archaeometry*, 60, 4, pp. 845–858.

Ali, M.F., El-Sheikha, A.M., Ali, A.E. (2016) Analytical Study and Conservation of Gilded Mummiform Cartonnage from the Greco-Roman Period in Cairo Museum, *Mediterranean Archaeology and Archaeometry,* Vol. 16, No 2, pp.127-137

Al-Emam, E., El-Gohary, M. and Abd El Hady, M. (2015) The paint layers of mural paintings at Abydos temples-Egypt: A closer look at the materials used*, Mediterranean Archaeology and Archaeometry*, Vol.15, issue.3, pp.113-121.

Bilal, S., Mohammed-Dabo, I.A., Dewu, B.M., Momoh, O. R., and Abubakar S. (2015) Refining and Characterization of Gum Arabic Using Vacuum Filtration Method for Application in Oil and Gas Drilling Fluid Formulation*, Journal of Experimental Research*, Vol. 3, issue.2, pp.73-80.

Borg, B.E. (2010) Painted Funerary Portraits. In Willeke Wendrich (ed.), UCLA Encyclopaedia of Egyptology, Los Angeles, California Digital Library University of California, 1(1), pp.1-12

Clark, R.J.H. and Curri, M.L. (1998) The identification by Raman microscopy and X-ray diffraction of iron-oxide pigments and of the red pigments found on Italian pottery fragments, *Journal of Molecular Structure,* Vol. 440, Issues 1–3, pp. 105-111 .

Coccato, A. (2017) *Application of Raman and X-ray fluorescence Spectroscopes to Cultural Heritage materials The non-destructive examination of paintings, pigment, and their degradation*, Thesis submitted in fulfilment of the requirements for the degree of Doctor of Archaeology, Faculty of arts and philosophy, Ghent University, Belgium, p.38.

Corcoran, L.H. (2014) Portrait mummy in roman Egypt (I-IV A.D.) with a catalogue of portrait mummy in Egyptian museum, (ed) Holland, T., Urban, T., *Studies in Ancient Oriental Civilization*, Oriental institute of the University of Chicago, Chicago, USA, no.56, p.30

Daniels, V., and Leach, B. (2004) The occurrence and alteration of realgar on Ancient Egyptian papyri, Studies in Conservation, Taylor & Francis, Ltd. on behalf of the International Institute for Conservation of Historic and Artistic Works, p. 49:73-84.

Daoubab, R.M.A., Aarif H.E., Mini, M.b., Elfatih, A.H. and Mohammed E.O. (2016) Characterization and functional proper- ties of some natural Acacia gums, *Journal of the Saudi Society of Agricultural*. Vol. 17, Issue 3, pp. 241-249

Dayet, L., Daniel, F., Guibert, P. and Jean Texier, P. (2013) Non-destructive analysis of archaeological ochre: a preliminary application to the Middle Stone Age site of Diepkloof Rock Shelter (South Africa), *Archaeometry*, Vol.1: e19, pp.89-94.

Derrick, M.R., Stulik, D. and Landry, J.M. (1999) *Infrared Spectroscopy in Conservation Science*, The Getty Conservation Institute, Los Angeles, p.179

Die-Stefano, L.M., & Fuchs, R. (2011) Characterizations of the pigments in a Ptolemaic Egyptian book of the dead papyrus, *Archaeo. Anthropol. Sci*,3, pp.229-224.

Dodson, A.M. (2011) Two Mummy-Masks from the Dawn of the New Kingdom- in D Aston (ed.), Under the Potter's Tree: Studies on Ancient Egypt Presented to Janine Bourriau on the Occasion of her 70th Birthday. Leuven, Belgium: Peeters, pp. 333–47

Elgaoudi, H., Varella, E., Kourkoumelis, N., and Kovala Demertzi, D. (2011) The effect of thermal aging and color pigments on the Egyptian linen properties evaluated by physicochemical methods, *Applied Physics A,* 105(2), pp.497-507.

Ferreira, L., Vega, S., Sánchez-Juanes, F., González, M., Herrero, A., Muñiz, M.C., González-Buitrago, J.M. and Muñoz, J.L. (2010) Identification by using MALDI-TOF mass spectrometry of lactic acid bacteria isolated from non-commercial yoghurts in southern Anatolia, Turkey, *Antimicrobial*, 20(1), pp.2530.

Gimenez, J. (2015) Egyptian blue and/or atacamite in an ancient Egyptian coffin, Vol. 6, Issue 4, pp.747-749. Gutman, M., Zanier, K., Lux, J. and Kramer, S. (2010) pigment analysis of Roman wall paintings from two villa rusticate in Slovenia, *Mediterranean Archaeology and Archaeometry*, Vol. 16, No. 3, pp. 193-206.

Hatton, G.D., Shortlandb, A.J. and Tite, M.S. (2008) The production technology of Egyptian blue and green frits from the second millennium BC Egypt and Mesopotamia, *Journal of Archaeological Science*, 35, pp. 1591-1604.

Hassaan, G.A. (2016) Mechanical Engineering in Ancient Egypt, Part XXX: Mummy Masks Industry, International Journal Of Advancement In *Engineering Technology, Management and Applied Science* (IJAETMAS), Volume 03, Issue 11, PP. 139-154 ISSN: 2349-3224.

Hussein, A.M., Madkor, F.S., Afifi, H.M., Abd-elghani, M. and Abd-Elfatah, M. (2019) Comprehensive study of an ancient Egyptian foot case Cartonnage using Raman, SEM-EDS, XRD and FTIR, *Vibrational Spectroscopy*, Vol. 106, pp.1-10

Iriarte, E., Foyo, A., Sanchez, M.A., and Tomillo, C. (2009) The origin and Geochemical characterization of red ochre's, *Archaeometry*, Vol.51, No 2, pp.231-251.

Mahmoud, H.M. & Papadopoulou, L. (2013) Archaeometric Analysis of Pigments from the Tomb of Nakht-Djehuty (TT189), El-Qurna Necropolis, Upper Egypt, *ArchéoSciences- revue d'archéométrie*, vol. 37, pp. 19-33.

Mahmoud, M.H.H. (2010) Preliminary Investigation Of Ancient Pigments From The Mortuary Temple Of Seti I, El- Qurna (Luxor, Egypt), *Mediterranean Archaeology and Archaeometry*, Vol. 11, No. 1, pp. 99-106.

Katsaros, T., Liritzis, L., Laskaris, N. (2010) Identification of Theophrastus' pigments Egyptian Kyanos and psimythion from an archaeological excavations: A case study, *ArchéoSciences, revue d'archéométrie*, 34, pp. 69-79 .

Mansur, M.A., Ali, M.F., Badr, N.M., Salem, M.Z. (2017) A Study of Bio-deterioration and Chromatic Alterations of Painted and Gilded Mummy Cartonnage at the Saqqara Museum Storeroom, Egypt'', *Archaeometry*, pp.4-14.

Cybulska, M. (2017) Archaeological Textiles–A Need for New Methods of Analysis and Reconstruction, *Fibres and Textiles in Eastern Europe,* 15, 5-6, pp.64-65

Mazzocchin, G.A., Rudello, D., Bragato, C. and Agnoli, F. (2004) A short note on Egyptian blue, *Journal of Cultural Heritage* 5, pp.129–133.

Montalto, N, A. (2010) *The characterization and provenancing of ancient ochre's,* PhD, Cranfield University, UK, p.4.

Moussa, A. (2013) comparative study of Egyptian blue fragments from Egypt and Tunisia, *Egyptian Journal of Archaeological and Restoration Studies "EJARS"*, Vol. 3, Issue 1, pp.13 - 19.

Moussa, A., And Ali, M.F. (2013) Colour Alteration of Ancient Egyptian Blue Faience, *International Journal of Architectural Heritage,* 7, pp.261–274.

Ni, M., Ratner., B.D. (2008) Differentiation of Calcium Carbonate Polymorphs by Surface Analysis Techniques - An XPS and TOF-SIMS study, *Surf Interface Anal*, 40(10), pp.1356-1361.

Pagès-Camagna, S., and Colinart, S. (2003) The Egyptian Green pigment: it's Manufacturing process and links to Egyptian Blue, *Archaeometry,* 45, pp.637-658.

Pagès-Camagna, S., Colinart, S. and coupry, C. (1999) Fabrication processes of archaeological Egyptian blue and green pigment enlightened by Raman microscopy and scanning electron microscopy, *Journal Raman Spectroscopy*, vol. 30, issue 4, pp. 313-317.

Panagopoulou, A., Karanasios, K. and Xanthopoulou, G. (2016) Ancient Egyptian Blue ($CaCuSi_4O_{10}$) Pigment by Modern Solution Combustion Synthesis Method, *Eurasian Chemical-Technological Journal*, 18, pp.31-37.

Hassan, R.R.A. (2019) Fourier transform infrared spectroscopy to detect thermal degradation of vegetable and chrome-tanned leather, *Spectroscopy Letters*, 52:5, 288-296. DOI: 10.1080/00387010.2019.1623262.

Scott, D.A., Dennis, M., Kandekar, N., Keeney, J., Carson, D. and Swartz Dodd, S. (2003) An Egyptian Cartonnage of the Greco-Roman Period: Examination and Discoveries, *Studies in Conservation*, Vol. 48, No. 1, pp. 41-56. DOI: 10.2307/1506822

Scott, D.A., Warmlander, S., Mazurek, J. and Quirke, S. (2009) Examination of some pigments, grounds and media from Egyptian Cartonnage fragments in the Petrie Museum, University College London, *Journal of Archaeological Science* 36, 923–932.

Siddall, R. (2006) Pigments and painting techniques of Roman Artist, *in Focus*, No 2, pp.20-31

Scott, P. (1998) Ancient faces: mummy portraits from Roman Egypt. Promoting the interdisciplinary study of death and dying, The British Museum, England, *J. of Mortality,* Vol. 3, Issue 2, pp. 195-196

Abd El kader, S., Hamed, M. and Hassan, R.R.A. (2019) Microscopic characterization of acidic paper manuscripts. *Pigment & Resin Technology*, Vol. 48 Issue.2, pp.119-128,

Taylor, J.H. (2001.) *Death and the Afterlife in Ancient Egypt*, London, British Museum Press for the trustees of the British museum, pp.10-45.

Tite, M.S. (1987) Characterizations of early vitreous materials, *Archaeometry*, pp.29, 21–3

Uda, M., Sassa, S., Yoshimura, s., J. Kondo, J., Nakamura., M., Ban, Y. and Adachi, H. (2000) Yellow, red and blue pigments from ancient Egyptian palace painted walls, *Nuclear Instruments and Methods in Physics Research B* 161-163, pp. 758-761.

https://www.researchgate.net/publication/229314852_Yellow_red_and_blue_pigment_from_ancient_Egyptian_palace_painted_walls

Wallis, E.A.D. (1899) Egyptian ideas of the future life, Osiris and the Egyptian Resurrection, London,, England, pp.2-60

Walker, R., Watkins, E., Tian, R., Bräu, L., O'Hara, G., Goodwin, L., Han, J., Reddy, T., Hunit, E. M., Pati, A., Woyke, T., Mavromatis, K., Markowitz., Ivanova, N., Kyrpides, N. and Reeve, W. (2014) Genome sequence of the acid-tolerant Burkholderia sp. strain WSM2232 from Karijini National Park, Australia, *Standards in Genomic Sciences,* 9, pp.1168-1180.

Hassan, R.R.A. (2016) preliminary study on using line seed oil emulsion in dressing archaeological leather *Journal of Cultural Heritage*, Vol. 21, 786-795.

Weatherhead, F., and Buckley, A. (1988) Artist's pigments from Amarna, Reports V, Egypt Exploration Society, London., pp.202- 240.